

# A test on analytic continuation of thermal imaginary-time data

Y. Burnier<sup>1</sup>, M. Laine<sup>2</sup>, and L. Mether<sup>2</sup>

<sup>1</sup> Dept. of Physics and Astronomy, SUNY, Stony Brook, New York 11794, USA

<sup>2</sup> Faculty of Physics, University of Bielefeld, D-33501 Bielefeld, Germany

Received: 3 February 2011 / Revised: 8 March 2011

**Abstract.** Some time ago, Cuniberti *et al* have proposed a novel method for analytically continuing thermal imaginary-time correlators to real time, which requires no model input and should be applicable with finite-precision data as well. Given that these assertions go against common wisdom, we report on a naive test of the method with an idealized example. We do encounter two problems, which we spell out in detail; this implies that systematic errors are difficult to quantify. On a more positive note, the method is simple to implement and allows for an empirical recipe by which a reasonable qualitative estimate for some transport coefficient may be obtained, if statistical errors of an ultraviolet-subtracted imaginary-time measurement can be reduced to roughly below the per mille level.

## 1 Introduction

It is a perennial problem that a reliable study of strong interactions at temperatures around a few hundred MeV requires non-perturbative methods, yet standard Monte Carlo techniques only work in Euclidean signature. This implies that many of the physically most interesting observables, such as transport coefficients or particle production rates (for reviews see e.g. refs. [1,2]), which are inherently Minkowskian in nature, are difficult to address.

A few years ago, a possible solution to this problem was proposed [3], through the use of a “Maximum Entropy Method” [4]. Unfortunately, despite many implementations and various related attempts (see e.g. refs. [5]–[11]; similar discussions continue also in the context of condensed matter physics problems, see e.g. ref. [12] and references therein), it remains a problem that there appears to be uncontrolled dependence on model input in these results. Therefore, it is perhaps worthwhile to look for alternatives as well.

Some time ago, Cuniberti *et al* [13] put forward a concrete suggestion which could help in this respect. An algorithm was provided which was shown to yield a correct analytic continuation in a specific limit; furthermore, it was suggested that the method might work even if there is a finite amount of data and the data points have error bars. Despite these attractive features, we are not aware of a previous numerical implementation of the algorithm. For the record, we wish to report one in this short note, even if quantitative success is somewhat marginal. Our hope is that some of our theoretical remarks are nevertheless of interest and that, on the qualitative level, the algorithm might turn out to be a useful addition to the existing tool kit.

## 2 Basic idea

The general philosophy of the method can be summarized as follows. We consider a periodic (“bosonic”) Euclidean correlator,  $\mathcal{G}(\tau, \cdot)$ , with  $\mathcal{G}(\tau + k\beta, \cdot) = \mathcal{G}(\tau, \cdot)$  where  $k \in \mathbb{Z}$ ,  $\beta$  denotes the inverse temperature, and  $\cdot$  denotes suppressed variables such as spatial momentum. The correlator should be analytic everywhere except at  $\text{Re } \tau = 0 + k\beta$ ; there it should still be continuous. We also assume the further property  $\mathcal{G}(\beta - \tau, \cdot) = \mathcal{G}(\tau, \cdot)$ ,  $0 < \tau < \beta$ , which was not imposed in ref. [13] but is satisfied by typical gauge-invariant current-current correlators measured in lattice QCD. Given the finiteness of  $\beta$ , the Fourier representation involves a discrete set of Matsubara frequencies,  $\tilde{\mathcal{G}}(\omega_n, \cdot) \equiv \int_0^\beta d\tau e^{i\omega_n \tau} \mathcal{G}(\tau, \cdot)$ ,  $\omega_n = 2\pi n T$ ,  $n \in \mathbb{Z}$ ,  $T \equiv \beta^{-1}$ . Making use of a general hypothesis about the asymptotic behaviour of various correlators in the Minkowskian time domain, namely that they show at most powerlike growth at infinity (physically relevant correlators are actually expected to vanish at infinity, see e.g. ref. [14]), a unique analytic continuation to a part of the complex plane can be shown to exist and can be constructed explicitly.

More concretely,<sup>1</sup> the basic quantities defined in ref. [13] are the one-sided sum  $\mathcal{G}^+(\tau, \cdot) \equiv T \sum_{\omega_n \geq 0} \tilde{\mathcal{G}}(\omega_n, \cdot) e^{-i\omega_n \tau}$ , which is analytic for  $\text{Im } \tau < 0$  but has cuts in the upper half-plane; its discontinuity across the cut starting at the origin,  $J^+(t, \cdot) \equiv i[\mathcal{G}^+(\epsilon + it, \cdot) - \mathcal{G}^+(-\epsilon + it, \cdot)]$ ,  $t > 0$ ,  $\epsilon = 0^+$ , which equals the retarded real-time correlator,  $\mathcal{R}(t, \cdot)$ ; as well as its Laplace transform  $\tilde{J}^+(\zeta, \cdot) \equiv \int_0^\infty dt e^{-\zeta t} J^+(t, \cdot)$ , which is analytic for  $\text{Re } \zeta > 0$ . For  $\zeta = \omega_n$ ,  $\tilde{J}^+(\zeta, \cdot)$  reduces to the Fourier

<sup>1</sup> The following relations, though simple to state, may not be entirely obvious at first sight; mathematical proofs can be found in ref. [13] and references therein.

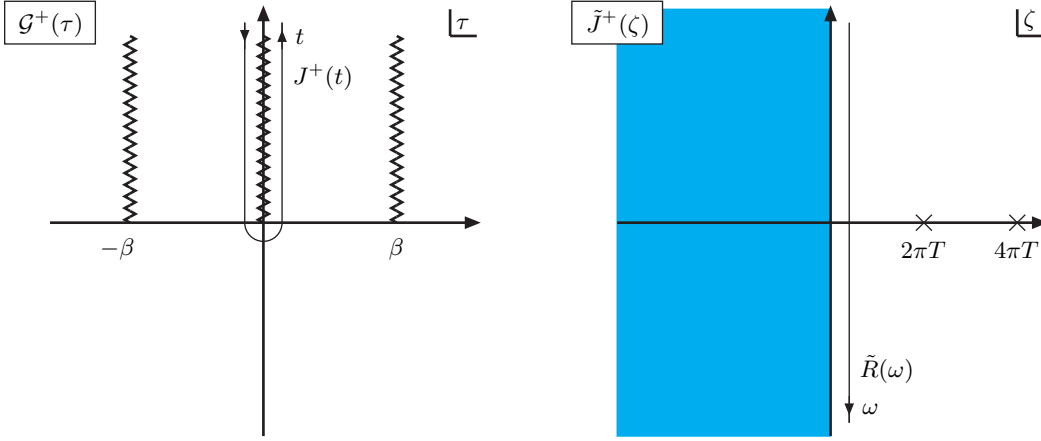


**Fig. 1.** The complex planes, basic functions, and analytic structures as discussed in the text.

components  $\tilde{\mathcal{G}}(\omega_n, \cdot)$ , and therefore constitutes the desired analytic continuation to a complex half-plane. The value of  $\tilde{J}^+(\zeta, \cdot)$  along the axis  $\zeta = \epsilon - i\omega$ ,  $\omega \in \mathbb{R}$ , yields the Fourier transform of the retarded correlator,  $\tilde{\mathcal{R}}(\omega, \cdot)$ , whose imaginary part in turn equals the spectral function. The basic analytic structure is illustrated in fig. 1.

### 3 Algorithm

To implement the analytic continuation, the idea of ref. [13] is to expand  $\tilde{J}^+(\zeta, \cdot)$  with the help of Pollaczek polynomials (of the type defined on an infinite interval); the retarded correlator  $J^+(t, \cdot)$  is in turn expressed as a linear combination of Laguerre polynomials, with argument  $2e^{-2\pi tT}$ . More explicitly, taking ref. [13] at face value, the steps are as follows:

- (i) Compute the Fourier modes,  $\tilde{\mathcal{G}}(\omega_n, \cdot)$ . Due to  $\mathcal{G}(\beta - \tau, \cdot) = \mathcal{G}(\tau, \cdot) \in \mathbb{R}$ , the Fourier modes are real and even in  $\omega_n \rightarrow -\omega_n$ .
- (ii) Construct the coefficients

$$a_\ell \equiv 2(-1)^\ell \sum_{n=0}^{\infty} \frac{(-1)^n}{n!} \tilde{\mathcal{G}}(\omega_{n+1}, \cdot) {}_2F_1(-\ell, n+1; 1; 2), \quad \ell = 0, 1, 2, \dots \quad (1)$$

We have re-expressed the Pollaczek polynomials of ref. [13] through the hypergeometric function  ${}_2F_1$ .<sup>2</sup> Note that the Matsubara zero-mode does not contribute in eq. (1).

- (iii) According to ref. [13],  $a_\ell$  decreases with  $\ell$ , such that  $\sum_{\ell=0}^{\infty} |a_\ell|^2$  is finite.
- (iv) Defining  $\tilde{t} \equiv 2\pi tT$ , the retarded real-time correlator can now be obtained as

$$J^+(\tilde{t}, \cdot) = e^{-e^{-\tilde{t}}} \sum_{\ell=0}^{\infty} a_\ell L_\ell(2e^{-\tilde{t}}), \quad (2)$$

<sup>2</sup> More precisely:  $P_\ell(\eta) \equiv P_\ell^{1/2}(\eta; \frac{\pi}{2}) = i^\ell {}_2F_1(-\ell, \frac{1}{2} + i\eta; 1; 2)$ , cf. ref. [15].

where  $L_\ell$  are the Laguerre polynomials. Given that  $L_\ell(0) = 1$ , the asymptotic value is  $J^+(\infty, \cdot) = \sum_{\ell=0}^{\infty} a_\ell$ , which should vanish in physically meaningful examples [14].

- (v) Given  $J^+$ , the spectral correlator reads  $\rho(t) = \frac{1}{2i} [\theta(t)J^+(t) - \theta(-t)\tilde{J}^+(-t)]$ , where  $\tilde{J}^+$  denotes a complex conjugate. Noting that  $J^+$  as produced by eq. (2) is real under our assumptions, the spectral function can finally be obtained as

$$\rho(\tilde{\omega}, \cdot) = \int_0^\infty d\tilde{t} \sin(\tilde{\omega}\tilde{t}) J^+(\tilde{t}, \cdot), \quad \tilde{\omega} \equiv \frac{\omega}{2\pi T}. \quad (3)$$

### 4 Practical implementation

To apply the previous algorithm to a situation where only a finite number of data points are available, we adopt the following steps, with the same numbering as in section 3.

- (i) We assume the interval  $0 < \tau < \beta$  to be evenly divided into  $N$  parts. The Fourier modes are constructed by a discrete transformation; we leave out the “contact point” ( $\tau = 0$  or  $\tau = \beta$ ), given its possible inaccessibility to practical measurement. Then,

$$\tilde{\mathcal{G}}(\omega_n, \cdot) \simeq \frac{\beta}{N} \sum_{k=1}^{N-1} e^{i\frac{2\pi nk}{N}} \mathcal{G}\left(\frac{k\beta}{N}, \cdot\right), \quad n = 0, \dots, N-1. \quad (4)$$

We stress again that, thanks to  $\mathcal{G}(\beta - \tau, \cdot) = \mathcal{G}(\tau, \cdot) \in \mathbb{R}$  for  $0 < \tau < \beta$ ,  $\tilde{\mathcal{G}}(\omega_n, \cdot) \in \mathbb{R}$ .

- (ii) Defining the coefficients  $\phi_{\ell, n} \equiv \frac{(-1)^\ell}{n!} {}_2F_1(-\ell, n+1; 1; 2)$ ,  $n \geq 0$ , which can be constructed from the recurrence relation

$$\begin{aligned} \phi_{\ell, -1} &\equiv 0; \quad \phi_{\ell, 0} = 1, \\ \phi_{\ell, n} &= \frac{(2\ell + 1)\phi_{\ell, n-1} + \phi_{\ell, n-2}}{n^2}, \quad n \geq 1, \end{aligned} \quad (5)$$

the  $a_\ell$  can be obtained from

$$a_\ell \simeq 2 \sum_{n=0}^{N-2} (-1)^n \tilde{\mathcal{G}}(\omega_{n+1}, \cdot) \phi_{\ell, n}. \quad (6)$$

The precise upper limit (be it  $N - 2$  or e.g.  $N/2$ ) has little importance, because  $\phi_{\ell,n}$  turn out to decrease rapidly for  $n > n_{\max}$ , where in general  $n_{\max} \ll N/2$  (cf. below).

- (iii) According to ref. [13], the  $|a_\ell|$  decrease only up to some  $\ell_{\max}$ , meaning that  $\sum_{\ell=0}^{\ell_{\max}} |a_\ell|^2$  shows a plateau as a function of  $\ell_{\max}$ , but eventually it diverges. Ref. [13] suggests choosing  $\ell_{\max}$  from this plateau. We find, however, that in practice it is more useful to monitor the sum  $\sum_{\ell=0}^{\ell_{\max}} a_\ell$ ; the reason is discussed in connection with eq. (9) below.
- (iv) Choosing  $\ell_{\max}$  according to some criterion,  $J^+$  can be approximated through

$$J^+(\tilde{t}, \cdot) \simeq e^{-e^{-\tilde{t}}} \sum_{\ell=0}^{\ell_{\max}} a_\ell L_\ell(2e^{-\tilde{t}}), \quad (7)$$

where, as usual, the  $L_\ell$  can be constructed from

$$\begin{aligned} L_0(x) &= 1, & L_1(x) &= 1 - x, \\ L_\ell(x) &= 2L_{\ell-1}(x) - L_{\ell-2}(x) \\ &\quad - \frac{(1+x)L_{\ell-1}(x) - L_{\ell-2}(x)}{\ell}, & \ell &\geq 2. \end{aligned} \quad (8)$$

In general the asymptotic value,

$$J^+(\infty, \cdot) = \sum_{\ell=0}^{\ell_{\max}} a_\ell, \quad (9)$$

does not vanish. In contrast, physically relevant current-current correlators should vanish at infinite time separation [14]. It turns out that this supplementary information can be used to choose values of  $\ell_{\max}$ , namely those for which  $J^+(\infty, \cdot)$  vanishes approximately, offering “windows of opportunity”, in which the algorithm appears to perform reasonably well even with non-ideal data.

- (v) The spectral function can be obtained as

$$\rho(\tilde{\omega}, \cdot) \simeq \int_0^\infty d\tilde{t} \sin(\tilde{\omega}\tilde{t}) \left[ J^+(\tilde{t}, \cdot) - J^+(\infty, \cdot) \right], \quad (10)$$

where we have subtracted by hand any possible “remnant”  $J^+(\infty, \cdot)$ . (Otherwise  $\rho(\tilde{\omega}, \cdot)$  would diverge as  $\sim 1/\tilde{\omega}$  at small frequencies.)

As the proofs in ref. [13] show, in the limit  $N \rightarrow \infty$  and vanishing errors these steps do yield the correct spectral function for current-current correlators of the considered type.

## 5 Problems

We now turn to two problems that limit the usefulness of the algorithm specified above. For simplicity the discussion will be carried out in the combined continuum and infinite-volume limit; a finite cutoff alleviates problem (i) but adds more structure to the spectral function and

thereby renders problem (ii) worse. A finite volume can in principle also change the behaviour of Euclidean correlators in a physically interesting way (cf. ref. [16] and references therein), however we wish to ignore these effects for now. (Formally a smooth infinite-volume type shape could be obtained e.g. by considering a suitable Gaussian smoothing of  $\rho(\omega, \cdot)/\omega$ .)

- (i) In order for the recipe to apply, we must be able to compute the Fourier coefficients  $\tilde{\mathcal{G}}(\omega_n, \cdot)$ ; this implies that  $\mathcal{G}(\tau, \cdot)$  must be integrable around  $\tau = 0 \bmod \beta$ . In fact, as mentioned above, in ref. [13]  $\mathcal{G}(\tau, \cdot)$  was even assumed to be continuous (and therefore finite) at  $\tau = 0 \bmod \beta$ . In contrast, the correlation functions of composite operators that are relevant for the determination of transport coefficients or particle production rates in QCD diverge at small  $\tau$  in the continuum limit.

In principle, a possible way around the problem might be to consider the temperature derivative of a correlator, rather than a correlator as such. This could work if the derivative is taken in fixed physical units. Sometimes, such differences are rather taken in scaled units, i.e. by subtracting values of  $\tilde{\mathcal{G}}(\hat{\tau}, \cdot) \equiv \beta^p \mathcal{G}(\hat{\tau}\beta, \cdot)$ ,  $0 < \hat{\tau} < 1$ , at different  $\beta$ 's, but such differences are continuous only if there are no scaling violations at small  $\tau$ .

In terms of a spectral function, the finiteness of  $\mathcal{G}(0^+, \cdot)$  necessitates  $\rho(\omega, \cdot) \leq C/(\omega \ln^2 \omega)$  at  $\omega \gg T$ , cf. eq. (12). The asymptotics of various spectral functions in this regime have been analyzed in ref. [17], and for vector current correlators the decay of the thermal part is indeed fast enough to satisfy the bound.

- (ii) As can be seen from eq. (6), the factor  $(-1)^n$  implies a cancellation between Fourier modes in the construction of the  $a_\ell$ 's; when the  $a_\ell$ 's multiply the Laguerre polynomials in eq. (7), further cancellations take place, particularly at large  $\tilde{t}$  (cf. eq. (9)). This implies a substantial significance loss. Furthermore, as can be seen from eq. (5), for a fixed  $\ell$  the coefficients  $\phi_{\ell,n}$  grow very fast at small  $n$ , reaching a maximal value at  $n_{\max} \approx \sqrt{2(\ell+1)}$ . The maximal value,  $\phi_{\ell, n_{\max}}$ , grows with  $\ell$ , exceeding  $10^4$  at  $\ell = 21$  (for  $n_{\max} = 6$ ),  $10^6$  at  $\ell = 40$  (for  $n_{\max} = 9$ ) and  $10^8$  at  $\ell = 64$  (for  $n_{\max} = 11$ ). So, the Fourier coefficients around  $n \sim n_{\max}$  would need to be determined with the corresponding relative accuracy in order to obtain a meaningful signal even after the cancellations. This is obviously a formidable challenge, particularly considering that problem (i) already requires a subtraction and inflicts an associated significance loss.

## 6 Test

Despite the problems of the previous section, we now wish to demonstrate that in principle the method may still work on the qualitative level. In order to achieve this, we assume that a suitable ultraviolet subtraction has been carried out, and that our data are quite precise.

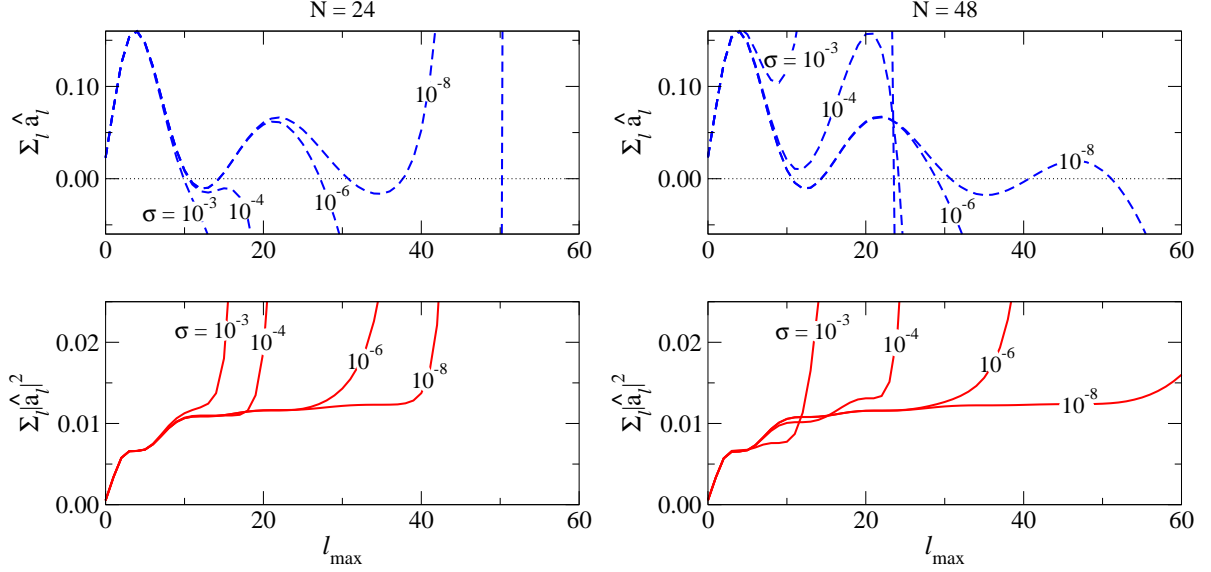


**Fig. 2.** Top:  $\sum_{\ell=0}^{\ell_{\max}} \hat{a}_\ell$  as a function of  $\ell_{\max}$ , for  $N = 24$  (left) and  $N = 48$  (right); here  $\hat{a}_\ell \equiv a_\ell/T^3$  and  $\sigma$  indicates the local relative standard deviation of  $\mathcal{G}(\tau, \cdot)$  (results are shown for one random configuration). Bottom: the corresponding  $\sum_{\ell=0}^{\ell_{\max}} |\hat{a}_\ell|^2$ .

As a model, we take inspiration from a spectral function related to an “electric field” correlator yielding the momentum-diffusion coefficient of a heavy quark [18, 19, 20]. We assume a substantial positive intercept of  $\rho(\omega, \cdot)/\omega$  at zero frequency (cf. ref. [21]) and decreasing behaviour at large frequency, just fast enough to yield a continuous  $\mathcal{G}(\tau, \cdot)$ :

$$\rho_{\text{test}} \equiv \frac{C \tilde{\omega}}{(2 + \tilde{\omega}^2)^2} \left[ 1 - \frac{\tilde{\omega}^2}{\ln^2(2 + \tilde{\omega}^2)} \right], \quad \tilde{\omega} \equiv \frac{\omega}{2\pi T}. \quad (11)$$

This spectral function is not positive-definite in order to reflect the fact that a suitable ultraviolet subtraction has been carried out, and because a negative  $\rho \sim -T^4/(\omega \ln^2 \omega)$  is precisely the qualitative asymptotic behaviour found in perturbation theory [22] (the logarithm squared assumes that the gauge coupling is let to run with  $\omega$ ).<sup>3</sup> The coefficient  $C$  appears linearly in all steps so that, without loss of generality, we set  $C \equiv 4T^3$  in the following, thereby normalizing  $\rho_{\text{test}}/(\tilde{\omega}T^3)$  to unity at  $\tilde{\omega} \rightarrow 0$ .

The Euclidean correlator is subsequently integrated numerically from

$$\mathcal{G}(\tau, \cdot) = \int_0^\infty \frac{d\omega}{\pi} \rho_{\text{test}} \frac{\cosh\left(\frac{\beta}{2} - \tau\right) \omega}{\sinh \frac{\beta \omega}{2}}, \quad (12)$$

for  $\tau = k\beta/N \leq \beta/2$ . At each  $\tau$  we add a random error from a Gaussian distribution of relative variance  $\sigma^2$ , and then mirror  $\mathcal{G}(\tau, \cdot)$  to the whole interval through the symmetry in  $\tau \rightarrow \beta - \tau$ . On this “data” the steps of section 4 are applied. Small variants of eq. (11) bring along little change, but the situation deteriorates rapidly if the structure is more peaked either in the ultraviolet ( $\omega \gg 2\pi T$ ) or in the infrared ( $\omega \ll 2\pi T$ ).

<sup>3</sup> Note that the Lorentzian form  $\rho \sim \tilde{\omega}/(\tilde{\eta}^2 + \tilde{\omega}^2)$  would not decrease fast enough at large frequencies.

The behaviour of the coefficients  $a_\ell$ , in particular the “diagnostic” sum of eq. (9), is illustrated in fig. 2; the quality of recovering the spectral function using windows of opportunity deduced from fig. 2 is shown in fig. 3. Fig. 4 demonstrates the effect of statistical noise on the final results. The lessons we draw are the following:

- (i) The recovery is reasonable only when  $\sum_{\ell=0}^{\ell_{\max}} a_\ell \approx 0$ . For good accuracy, the sum  $\sum_{\ell=0}^{\ell_{\max}} a_\ell$  shows a near-zero minimum; then  $\ell_{\max}$  should be chosen close to the minimum (the function  $\rho(\omega, \cdot)/\omega$  is also extremal there). For poor accuracy it could happen that no clear minimum is seen, cf.  $\sigma = 10^{-3}$  in fig. 2(left); then  $\ell_{\max}$  should be chosen close to a point where  $\sum_{\ell=0}^{\ell_{\max}} a_\ell$  crosses zero.
- (ii) Other values of  $\ell_{\max}$  lead in general to nonsensical results.
- (iii) Within a given “robust” near-zero minimum, the dependence on  $N$  and  $\sigma$  is quite mild.
- (iv) The recovery can be qualitatively improved only by increasing the accuracy so much that a second window opens up (cf.  $\sigma = 10^{-8}$  in fig. 2). This is unlikely to be reached in practice and, in any case, the improvement is not that overwhelming (cf. fig. 3).
- (v) The statements above apply to any single random configuration. With a sample of them,  $\ell_{\max}$  could be separately fixed for each configuration. Within our toy model, it requires an accuracy  $\sigma \lesssim 10^{-4}$  to find a useful minimum for almost every configuration (cf. fig. 4). For  $\sigma = 10^{-3}$ , typical configurations show no near-zero minimum (cf. fig. 2), but rare ones do and if it is possible to restrict the statistics to those and to carry out the averaging on the final  $\rho(\omega, \cdot)/\omega$ , then a rough estimate can still be obtained.

Although it goes beyond the scope of the present note to carry out a detailed investigation of issues related to

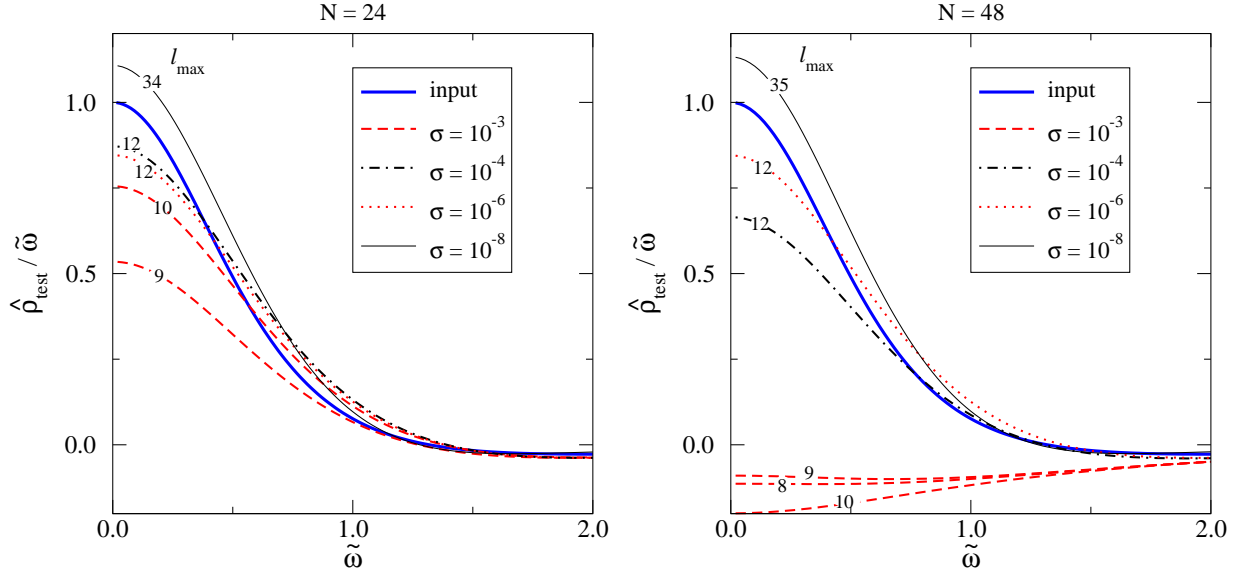


**Fig. 3.**  $\hat{\rho}_{\text{test}}/\tilde{\omega} \equiv \rho_{\text{test}}/(\tilde{\omega}T^3)$  as a function of  $\tilde{\omega} = \omega/(2\pi T)$ , for various relative accuracies  $\sigma$ , as well as  $\ell_{\text{max}}$  chosen from “windows of opportunity” in which  $\sum_{\ell=0}^{\ell_{\text{max}}} \hat{a}_{\ell}$  approximately vanishes, cf. fig. 2 (results are shown for one random configuration). The thick solid line is the correct (input) result. The case  $\sigma = 10^{-3}$  with  $N = 48$  shows a “failed” example: there is a minimum in  $\sum_{\ell=0}^{\ell_{\text{max}}} \hat{a}_{\ell}$  but it is not near zero (cf. fig. 2).

statistical analysis, we note that, in general, the output function depends non-linearly on input data, because the value of  $\ell_{\text{max}}$  varies and affects significantly the result. Error estimation should therefore be carried out with e.g. jackknife or bootstrap methods, perhaps with blocked configurations (the effect of blocking has been shown to be beneficial in connection with the Maximum Entropy Method, see e.g. ref. [23]).

## 7 Conclusions

The algorithm of ref. [13] possesses a number of attractive features: it can be fully specified in a small number of explicit steps; it requires no priors; it does not necessitate a positive-definite spectral function; and it projects out the Matsubara zero-mode contribution whose handling has been considered a problem in certain contexts.

Unfortunately, from a practical point of view, the algorithm of ref. [13] cannot be guaranteed to yield a quantitatively accurate analytic continuation of thermal imaginary-time data. In some sense, the situation is akin to the sign problem hampering simulations of QCD with a finite baryon number density: there are significant cancellations taking place, particularly if a spectral function at a small frequency  $\omega \ll 2\pi T$  needs to be determined. Also, short-distance divergences need to be subtracted from the Euclidean correlator  $\mathcal{G}(\tau, \cdot)$ , which constitutes a significance loss of its own.

Nevertheless, we have demonstrated that in a lucky case with a structureless spectral function and precise data (with relative errors  $< 0.1\%$  after the ultraviolet subtraction), already  $N \gtrsim 20$  data points may yield a qualitative reproduction of a transport coefficient (zero-frequency intercept of  $\rho(\omega, \cdot)/\omega$ ). In general, it is difficult to estimate

systematic errors, but if a clear near-zero minimum in  $\sum_{\ell=0}^{\ell_{\text{max}}} a_{\ell}$  is found as a function of  $\ell_{\text{max}}$ , then it appears that a  $\lesssim 50\%$  uncertainty can be expected. This could already be useful, given that current model-independent determinations of transport coefficients might contain errors of more than 100% [21].

## Acknowledgements

M.L. thanks Dietrich Bödeker for informing him about ref. [13] several years ago, and Harvey Meyer for useful discussions. M.L. was partly supported by the BMBF under project *Heavy Quarks as a Bridge between Heavy Ion Collisions and QCD*; L.M. was supported by the Alexander von Humboldt foundation and the Academy of Finland.

## References

1. G. Aarts, *Transport and spectral functions in high-temperature QCD*, PoS LAT2007 (2007) 001 [0710.0739].
2. H.B. Meyer, *Energy-momentum tensor correlators and viscosity*, PoS LATTICE2008 (2008) 017 [0809.5202].
3. M. Asakawa, T. Hatsuda and Y. Nakahara, *Maximum entropy analysis of the spectral functions in lattice QCD*, Prog. Part. Nucl. Phys. 46 (2001) 459 [hep-lat/0011040].
4. M. Jarrell and J.E. Gubernatis, *Bayesian inference and the analytic continuation of imaginary-time quantum Monte Carlo data*, Phys. Rep. 269 (1996) 133.
5. S. Gupta, *The electrical conductivity and soft photon emissivity of the QCD plasma*, Phys. Lett. B 597 (2004) 57 [hep-lat/0301006].
6. A. Jakovac, P. Petreczky, K. Petrov and A. Velytsky, *Quarkonium correlators and spectral functions at zero*

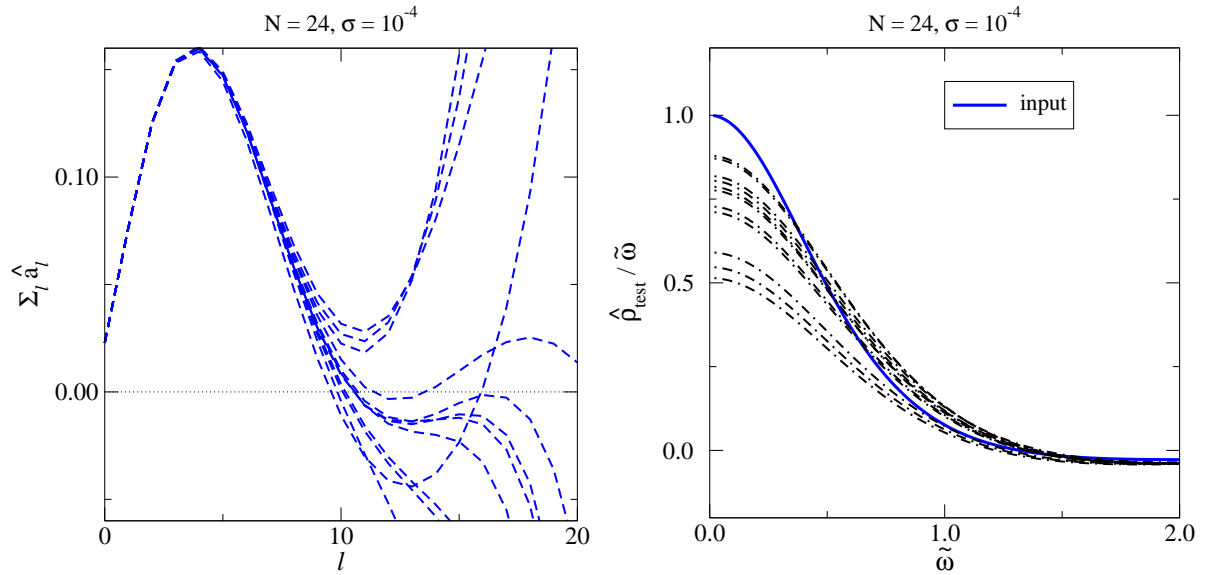


**Fig. 4.** Results from a sample of random configurations at  $N = 24$ ,  $\sigma = 10^{-4}$ , for  $\sum_{\ell=0}^{\ell_{\max}} \hat{a}_\ell$  (left) and  $\rho_{\text{test}}/(\tilde{\omega}T^3)$  (right). The parameter  $\ell_{\max}$  was chosen according to the criteria specified in the text, and varies within the range 10 – 13. The three lowest-most curves in the right panel correspond to the three cases in the left panel in which  $\sum_{\ell=0}^{\ell_{\max}} \hat{a}_\ell$  does not cross zero; omitting such configurations from the statistics would appear to reduce the systematic error of the final average.

- and finite temperature, Phys. Rev. D 75 (2007) 014506 [hep-lat/0611017].
7. G. Aarts, C. Allton, J. Foley, S. Hands and S. Kim, *Spectral functions at small energies and the electrical conductivity in hot, quenched lattice QCD*, Phys. Rev. Lett. 99 (2007) 022002 [hep-lat/0703008].
  8. H.B. Meyer, *A calculation of the shear viscosity in SU(3) gluodynamics*, Phys. Rev. D 76 (2007) 101701 [0704.1801].
  9. A. Rothkopf, T. Hatsuda and S. Sasaki, *Proper heavy-quark potential from a spectral decomposition of the thermal Wilson loop*, PoS LAT2009 (2009) 162 [0910.2321].
  10. J. Engels and O. Vogt, *Longitudinal and transverse spectral functions in the three-dimensional O(4) model*, Nucl. Phys. B 832 (2010) 538 [0911.1939].
  11. H.T. Ding, A. Francis, O. Kaczmarek, F. Karsch, E. Laermann and W. Soeldner, *Thermal dilepton rate and electrical conductivity: An analysis of vector current correlation functions in quenched lattice QCD*, Phys. Rev. D 83 (2011) 034504 [1012.4963].
  12. O. Gunnarsson, M.W. Haverkort and G. Sangiovanni, *Analytical continuation of imaginary axis data for optical conductivity*, Phys. Rev. B 82 (2010) 165125 [1012.5934].
  13. G. Cuniberti, E. De Micheli and G.A. Viano, *Reconstructing the thermal Green functions at real times from those at imaginary times*, Commun. Math. Phys. 216 (2001) 59 [cond-mat/0109175].
  14. P.B. Arnold and L.G. Yaffe, *Effective theories for real-time correlations in hot plasmas*, Phys. Rev. D 57 (1998) 1178 [hep-ph/9709449].
  15. G. Szegő, *Orthogonal Polynomials* (Amer. Math. Soc., Providence, RI, 1939).
  16. L. Lellouch and M. Lüscher, *Weak transition matrix elements from finite-volume correlation functions*, Commun. Math. Phys. 219 (2001) 31 [hep-lat/0003023].
  17. S. Caron-Huot, *Asymptotics of thermal spectral functions*, Phys. Rev. D 79 (2009) 125009 [0903.3958].
  18. J. Casalderrey-Solana and D. Teaney, *Heavy quark diffusion in strongly coupled N = 4 Yang Mills*, Phys. Rev. D 74 (2006) 085012 [hep-ph/0605199].
  19. S. Caron-Huot, M. Laine and G.D. Moore, *A way to estimate the heavy quark thermalization rate from the lattice*, JHEP 04 (2009) 053 [0901.1195].
  20. H.B. Meyer, *The errant life of a heavy quark in the quark-gluon plasma*, New J. Phys. 13 (2011) 035008 [1012.0234].
  21. S. Caron-Huot and G.D. Moore, *Heavy quark diffusion in QCD and N = 4 SYM at next-to-leading order*, JHEP 02 (2008) 081 [0801.2173].
  22. Y. Burnier, M. Laine, J. Langelage and L. Mether, *Colour-electric spectral function at next-to-leading order*, JHEP 08 (2010) 094 [1006.0867].
  23. O. Gunnarsson, M.W. Haverkort and G. Sangiovanni, *Analytical continuation of imaginary axis data using maximum entropy*, Phys. Rev. B 81 (2010) 155107 [1001.4351].